Simulation of the Saturnian magnetospheric interaction with Titan

Stephen H. Brecht

Bay Area Research Corporation, Orinda, California

Janet G. Luhmann

Space Sciences Laboratory, University of California, Berkeley

David J. Larson

Bay Area Research Corporation, Orinda, California

Abstract. Flowing plasma interactions with small bodies in the solar system are frequently complicated by the significant size of the ion gyroradii relative to the scale size of the body and the interaction region. This situation often applies to both the flowing ion populations and the atmospheric pickup ions added to the flow in the vicinity of the body. Titan represents an important example of this type of system and is scheduled to be probed in some detail during the Cassini mission tour of Saturn. Initial results from global hybrid (particle ions, fluid electrons) numerical simulations of Saturn's magnetospheric plasma encountering Titan's ionosphere reveal the complexity of the interaction introduced by the ion kinetics. The scale of the interaction region is dominated by the heavy ion gyroradii of the ambient and pickup ions rather than the size of Titan and is found to depend on the mass loading of the magnetospheric flow encountering Titan. Comparison with data from the Voyager 1 flyby suggests that ion kinetics as well as the relative orientations of external plasma ram and pickup ion production regions affect what was observed.

1. Introduction

The interaction of flowing magnetized plasma with the atmospheres of planets and moons that possess little or no intrinsic magnetic field is an area of intense research in the space physics community. The interactions occur for a wide variety of incident flow speeds and other plasma and field parameters as well as for different atmospheric/ionospheric densities and compositions. The flowing plasma and magnetic field interact directly with the ionospheres and neutral atmospheres of these objects in a comet-like fashion. However, the relatively small obstacles presented by these bodies give these systems strong elements of kinetic behavior that cannot be ignored.

In the case of Venus at its 0.7 AU heliocentric distance, the gyroradius of the solar wind ions does not significantly affect the hydrodynamic view of the interaction commonly used to describe the interaction of the solar wind with the ionosphere [*Moore et al.*, 1991a]. Nevertheless, the O^+ ions picked up by the solar wind convection electric fields, with gyroradii of the order of the planet radius, $R_V \cong 6350$ km, produce some asymmetries in the system, requiring a kinetic approach for this part of the interaction [*Moore et al.*, 1991b]. Venus has a classical bow shock, and Pioneer Venus Orbiter (PVO) data confirm that the great bulk of the incident solar wind is diverted around the obstacle created by the shielding currents induced in the ionosphere. Mars is not as well protected from the solar wind flow because the size of the solar wind ion gyrad-

ius is significant relative to the subsolar shock distance [*Brecht and Ferrante*, 1991] and the ionosphere is typically too weak to provide sufficient shielding currents [e.g., *Zhang and Luhmann*, 1992]. Indeed, recent research [*Brecht*, 1997a] suggests that a significant fraction of the solar wind ions are deposited directly into the Martian atmosphere.

Comparisons between Venus' magnetotail and that of Mars using observations from PVO and Phobos 2 indicate that Mars' tail region has a large-scale, draped magnetic structure similar to that at Venus [e.g., *Luhmann et al.*, 1991]. Ion measurements at Mars indicate the presence of a midtail lobe plasma sheet composed of suprathermal atmospheric O^+ ions [*Lundin et al.*, 1990a; *Dubinin et al.*, 1991] as well as a dayside O^+ ion mantle [*Breus et al.*, 1991] that may extend into a heavy ion tail boundary layer [*Lundin et al.*, 1990b]. The Voyager 1 data from Titan's wake give a similar overall impression [*Gurnett et al.*, 1982; *Hartle et al.*, 1982; *Ness et al.*, 1982], but the nature of the incident plasma flow and the greater extent of the Titan atmosphere relative to the body size make this interaction somewhat different in character. While the magnetic field measurements from Voyager 1 show that the gross magnetotail structure of Titan is similar to the magnetotails of Venus or Mars [cf. *Ip*, 1992], *Neubauer* [1992] thought the Titan data suggested a four-lobe tail structure rather than the usual two lobes expected for simple draping or an internal dipole. Our understanding of the physics of the Titan wake and its structure is very limited at present, and the single flyby at ~2.5 Titan radii downstream by Voyager 1, while tantalizing, limits our observational picture.

The Titan interaction with the magnetospheric plasma of Saturn is thought to be one in which substantial interpenetration occurs between the magnetospheric plasma and the atmosphere with associated energy deposition. As such, Titan provides an example

where the effects of external fields and plasma are of critical importance to the dynamics of the planetary atmosphere. Because Titan is usually within the Saturnian magnetosphere, the plasma and magnetic field incident upon Titan's atmosphere is typically a sub-Alfvénic flow. The major magnetospheric plasma constituents are H^+ and O^+, but at the orbit of Titan (20 Saturn radii) there is a nitrogen torus from Titan itself. The heavy pickup ions (N^+, N_2^+, H_2CN^+, $C_2H_5^+$) can have gyroradii that are 2-3 times the Titan radius, R_T, which is ~2575 km [Neubauer, 1992; Ip, 1990a]. Both magnetospheric electron impact ionization and photoionization are expected to play a role in producing Titan's ionosphere [Keller et al., 1992, 1994]. The Titan interaction also features the possibility of having its densest ionosphere on a face not aligned with the ram flow of the magnetosphere plasma if sunlight is a major source.

The research reported in this paper was directed toward obtaining some initial understanding of the Titan interaction with Saturn's magnetosphere. The main issues addressed are the effect of mass loading of the external plasma flow and magnetic field by Titan ionospheric ions and the interaction between the flow and Titan's ionosphere when the photoionization and magnetospheric electron impact ionization sources are not collocated. Comparisons between the results of the simulations and the Voyager I data along the flyby trajectory suggest that some of the structure and asymmetry in the wake observed on Voyager 1 is probably due to a combination of the relative scale sizes of the ion gyroradii and Titan and a dominant photoionization source. The results should be of particular interest to Cassini mission experimenters planning future Titan flybys.

2. Simulations

Simulation has been used for years to obtain both quantitative and detailed information about the interaction of planets with the solar wind. MHD simulations have been used for Earth and other planets having a significant intrinsic magnetic field that increases their effective obstacle size. In the case of Venus both MHD and gas dynamic models have been used to study such issues as the location of the Venusian shock as a function of ionospheric mass loading due to solar cycle variations [e.g., see Luhmann et al., 1997, and references therein]. However, fluid models, whether gas dynamic or MHD, cannot describe the physics when the scale size of interest is comparable to the ion gyroradius. In such cases there is both imperfect deflection of flow around the obstacle presented by the planet or body as well as significant asymmetry in the interaction regardless of whether the flow is super- or sub-Alfvénic/magnetosonic.

Recently, hybrid particle simulations (particle ions and fluid electrons) have been used to study the interaction of the solar wind with both Venus and Mars [cf. Brecht, 1990, 1997a b; Brecht and Ferrante, 1991; Brecht et al., 1993]. This simulation tool retains the full kinetic behavior of all ion species placed in the simulation, treats the electrons as a massless neutralizing fluid, and treats the particles and fields self-consistently. For the parameters of interest the speed of light is much larger than V_A, the Alfvén speed, so that the Darwin approximation of neglecting the transverse displacement current is valid.

With these approximations the model equations become Ampere's law,

$$\nabla \times \mathbf{B} = (4\pi/c)\,\mathbf{J}, \qquad (1)$$

where $\mathbf{B}$ is the magnetic field, c is the velocity of light, and $\mathbf{J}$ is the current density; Faraday's law,

$$c\nabla \times \mathbf{E} = -\partial \mathbf{B}/\partial t, \qquad (2)$$

the ion particle equations of motion m_i,

$$m_i\,d\mathbf{v}_i / dt = q_i\,\mathbf{E} + q_i\,\mathbf{v}_i \times \mathbf{B}/c - q_i\,\eta\,\mathbf{J}, \qquad (3)$$

$$d\mathbf{x}_i / dt = \mathbf{v}_i, \qquad (4)$$

where q_i is ... and $\mathbf{v}_i$ is ...; the inertialess electron momentum equation,

$$0 = -e\,n_e\,\mathbf{E} + \mathbf{J}_e \times \mathbf{B}/c - \nabla p_e + e\,n_e\,\eta\,\mathbf{J}, \qquad (5)$$

where n_e is ... and p_e is ...; and the requirement of quasi-neutrality,

$$n_e = n_i, \qquad (6)$$

for scale lengths greater than the Debye length. The equations are solved with a predictor-corrector method first published by Harned [1982]. The boundary conditions for these simulations are as follows: inflow of plasma and fields on the top boundary and outflow of particles and fields on all other outside boundaries. This is done with a technique that produces no reflections. The moon itself is assumed to be a conducting sphere (not a critical assumption since the ionosphere included carries much of the current). All particles that encounter the surface of the moon are removed from the simulation. Full details of the hybrid formalism including the equations solved are given by Brecht and Thomas [1988].

There are a variety of differences between a hybrid particle code and the MHD codes being used to simulate Titan [e.g. Ledvina and Cravens, 1998; Kabin et al., 1999]. Most of the MHD codes are single species (see (3), (4), and (5)) and do not carry the Hall term (second term of (5)). Therefore the MHD codes do not display diamagnetic effects and must return symmetric solutions. The effects of ion gyration are not simulated (see (3) and (4)). However, owing to its fluid nature, the MHD codes are better able to accommodate ionospheric chemistry, which is usually treated in a fluid approximation. Finally, they can cover larger regions where ion gyroradius effects and asymmetries due to Hall effects are not considered important. The hybrid model results presented here focus on the kinetic interaction of the global plasma interaction and, in particular, on the ionosphere/ion wake relationship.

The three-dimensional (3-D) HALFSHEL hybrid simulations used in the Titan case are essentially the same as those used for Mars but with the following parameters. The size of the numerical grid was 66 x 153 x 91 cells. The grid extent was 15 R_T x 30 R_T x 17.5 R_T, resulting in cell sizes of ~500 km in each direction. The simulations used roughly 12 million particles and 20 processors in the NASA Ames Numerical Aerodynamic Simulation Facility (NAS) Origin 2000 parallel computers. The external flow parameters used in these simulations were a cold magnetospheric plasma density of 0.2 particles cm^{-3} of N^+ at a velocity of 125 km s^{-1}. The choice of N^+ rather than a combination of H^+ and N^+ was dictated by the difficulty of properly handling multiple ion inflow conditions and the realization that N^+ carries most of the momentum. The magnetic field was set to 5.1 nT perpendicular to the flow, and ionospheric ions of various species (described below) were placed into the simulation at regular time intervals with an initial spatial distribution based on Titan ionosphere models.

The ionospheric production rates and ion densities are modeled in a simplified way because the limited spatial resolution of 500 km does not allow detailed simulation of the ionosphere itself. Particles are loaded with density weight sufficient to reproduce an ion density profile. The profile used was obtained from Figure 6 of Keller et al. [1992]. This profile is assumed; it is not self-consistently computed, the assumption being that we are starting the simulation from a mature state of the ionosphere. The profile is replenished on a time-dependent basis. Thus the inner ionosphere

"builds" up as the simulation proceeds. The choice of replenishment time is determined by the number of time steps it takes for a particle to move a cell at a fraction of the magnetospheric flow velocity. It is assumed that the chemistry would be doing this on timescales short compared to the simulation period (a few minutes). Hence there is no chemistry in these simulations. The code is capable of handling charge exchange, impact ionization, and collisions, but, as noted above, our spatial resolution in these initial simulations does not warrant a detailed treatment of the ionization mechanisms except insofar as they affect the global production geometry with respect to the plasma ram face. For similar reasons the results are not expected to yield reliable information about the ionospheric flows and related electric fields. However, the final pickup velocity should be reasonably accurate once the ions get into the magnetospheric flow.

The density profile used to load the ionospheric ions is actually an average for the multiple hydrocarbon species in the model of *Keller et al.* [1992]. This single density profile of $C_2H_5^+$ is used as an approximation of the possible hydrocarbon species. We chose $C_2H_5^+$ because according to *Keller et al.* [1992], it is the dominant contributor to the ionospheric mass loading at higher altitudes. Further, it offered the largest gyroradii of any of the ions. The model profile included the H_2CN^+ and CH_5^+ profiles. Their mass density was normalized to that of $C_2H_5^+$, so that the profile was representative of these species density and mass but is represented by a single species $C_2H_5^+$. It is not necessary to limit the code to one ionospheric species, but it makes the comparison of interest easier to perform. The next level of work will include better spatial resolution and multiple ions. The loaded profiles extended out to beyond 2500 km in altitude, where the exospheric ion density is less than 10% of the incoming flow mass density. While the more extended exosphere of Titan may mass load the magnetospheric flow before interaction with the main ionosphere, the dominant interaction effects will be due to the latter.

Separate ionospheric species were loaded into different simulations to evaluate the effect of pickup ion mass and gyroradii. The selected ions, H^+, N^+, and $C_2H_5^+$, were chosen because they represent the range of possibly dominant species in the upper ionospheric regions according to calculations by *Keller et al.* [1992, 1994]. The simulations with H^+ and N^+ representing the ionosphere instead of $C_2H_5^+$ were loaded with the same number density profile and thus not the same mass density profile. This assumption provided a sense of the importance of the pickup ion gyroradius without the complication of also having species-dependent scale heights.

The density profile for $C_2H_5^+$ was loaded at a rate such that by 5000 steps the density of the profile was ~10% of the full ionosphere profile calculated by *Keller et al.* [1992]. This was done because of the spatial resolution currently used in these simulations. With the 500-km cell size the peak region of the ionosphere is effectively averaged out. Therefore it was not appropriate to load the full ionosphere values calculated by *Keller et al.* [1992]. On the planetary "surface" the ion density is taken to be zero. The adjacent cell includes the ionospheric peak, followed by the next cell at 1000-km altitude, which contains densities several orders of magnitude smaller.

To mimic the possible effects of a combination of magnetospheric electron impact and photoionization sources of Titan pickup ions, we assumed an overall weak production rate of ~10% of the peak profile loaded and a hemisphere of primary production that could be moved with respect to the ram face. The production in the primary production hemisphere was assumed to fall off linearly with angle from the primary production region. The falloff stopped at a level of 10% of the peak.
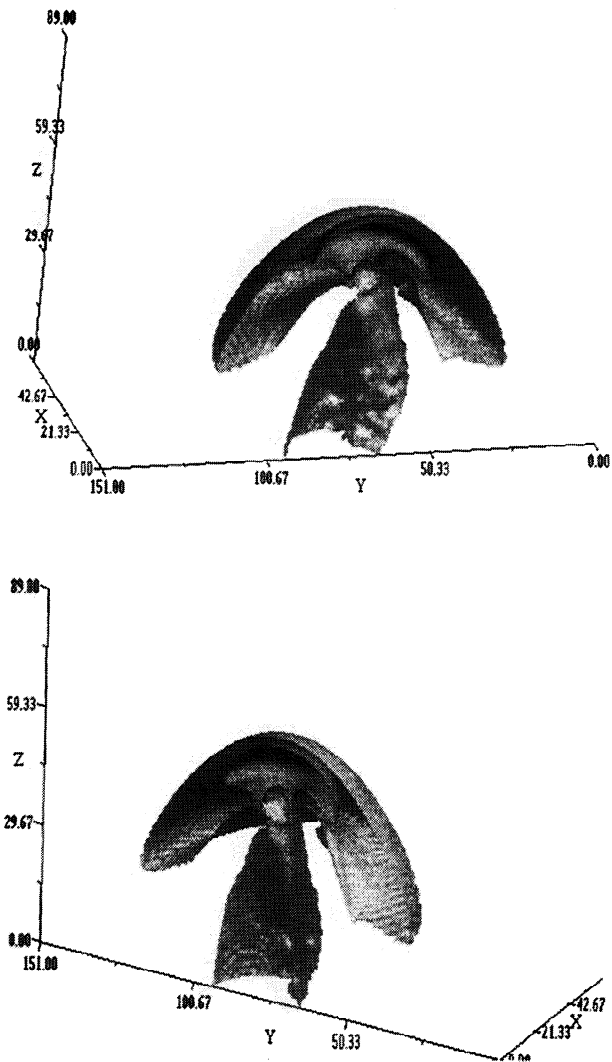

Figure 1. Three-dimensional surface plots of the magnitude of B around Titan. The magnetic field is in the x direction, the flow is in the $-z$ direction, and the convection electric field is in the $+y$ direction.

3. General Flow and Fields: Symmetric Loading

Understanding the possible magnetic topologies surrounding Titan was a major goal of this research. The 3-D HALFSHEL simulations provide some insight into this topology. The simulations described in this subsection assumed that the impact ionization and the photoionization peak regions are collocated with the magnetosphere ram flow face. Figure 1 shows, as three-dimensional surface plots of total field strength, two perspectives of the magnetic topological features typically found in these simulations. This figure has been cut along the convection electric field plane through the middle of Titan (in our simulations the $+y$ direction is the direction of the convection electric field, $E_{conv} = - V \times B$ where V and B are the velocity and magnetic field vectors, respectively). The flow is in the $-z$ direction, and the magnetic field is in the $+x$ direction. The major feature is a relatively symmetric bow wave "cap." Within this region a strong magnetic field pileup is found. While the general behavior is similar to that obtained in the global MHD models of *Ledvina and Cravens* [1998] and *Kabin et al.* [1999], this region is not symmetric and is seen to be more prominent in the direction of the convection electric field, $+y$ ($+ E_{conv}$). Further, the tail region is not aligned with the flow but is offset
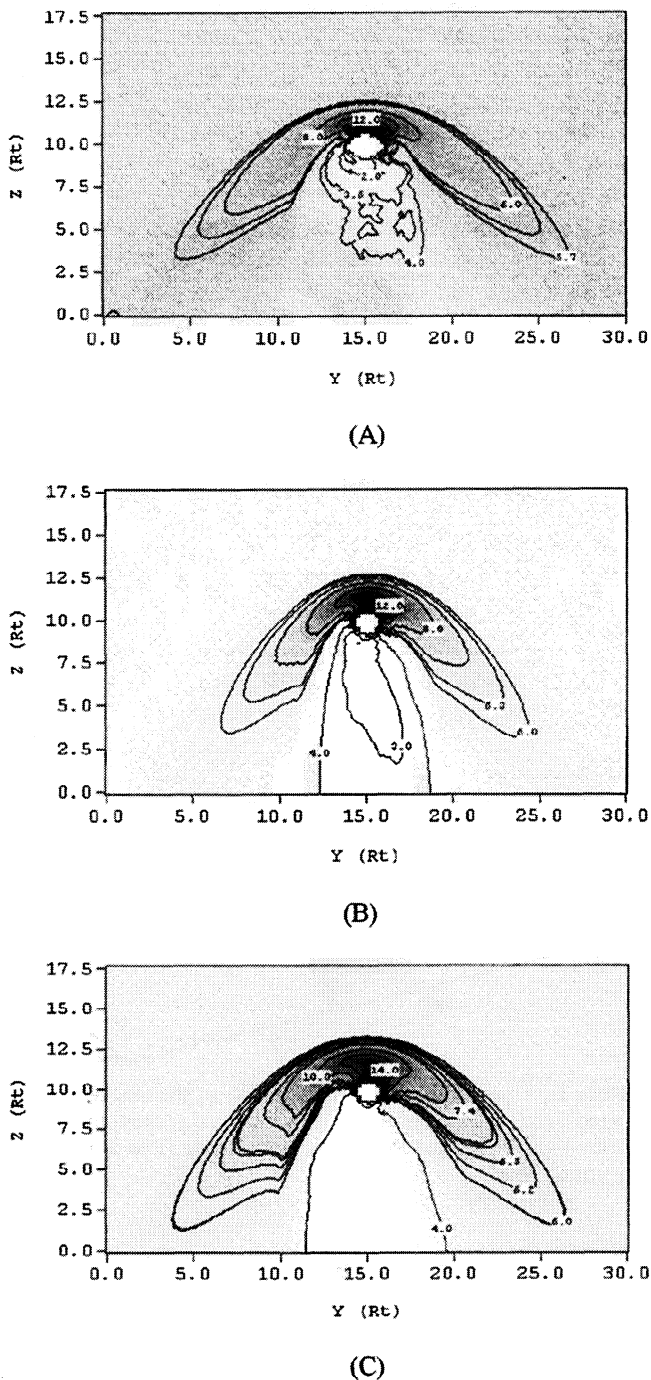
(A)

(B)

(C)

Figure 2. Contour plots of the magnitude of B (nT) for (a) H+ load, (b) N+ load, and (c) $C_2H_5^+$ load. This plane has the flow and convection electric field in it.

toward the + E_{conv} side of Titan. The asymmetric magnetic barrier and the offset of the tail region are caused by the diamagnetic currents from the multiple component plasma.

The effect of different pickup ion masses can be seen in the 2-D total field contours in Figures 2a-2c. These figures show cuts through the middle of Titan as in Fig. 1. The plane of the contours contains the convection electric field and the Saturn magnetospheric plasma flow vector. The magnetic field points out of the plane toward the reader. The scales are in Titan radii, R_T. A very smooth outer region of the bow wave (not shock) is present. The

maximum magnetic field is found in the nose region. Typically, it is in the 15 to 20 nT range, 3-4 times the ambient field strength. Figure 2a shows the magnitude of B following mass loading of H^+ around the planet. Figure 2b shows the results for a N^+ load. Finally, the $C_2H_5^+$ loaded simulation is shown in Figure 2c.

These figures illustrate that the mass of the ionospheric ions does make a major difference in the overall magnetic field topology around Titan. The heavier is the mass of the ions, the wider is the tail structure, which ranges from $\gtrsim 5 R_T$ for the H^+ case to 10 R_T for the $C_2H_5^+$ case when measured ~10 R_T downstream from Titan. Within the tail region there are significant fluctuations. The H^+ loaded case shows a much stronger level of turbulence and a less defined tail region but appears much smoother in the outer regions. In Figure 3 the plane containing the magnetic field and flow vector is shown. The result shown in this figure is representative of the three cases examined. A very smooth outer region of the bow wave is seen in all cases. The field is seen to stand off from the surface of the moon owing to the mass loading by the ionospheric ions and their current system. In the tail region there is again some wave activity but not to the extent seen in the orthogonal plane.

The total ion density can be viewed in the same manner as the magnetic field magnitude. Figures 4a-4c show the total ion density (inflowing and pickup ions) for the three mass loading cases progressing from light mass to heavy mass. The ion density plots show in a clearer fashion the impact made by the mass loading of the different species. The H^+ case shows very clear boundaries in the tail region. In these simulations we see pickup on both sides, but the most extensive pickup is on the + E_{conv} side. This is clear from the low density on this side of Titan. The peak mass densities are found in a narrow shell. On the opposite side of the tail one sees a clean boundary. As can be seen in Figure 4b, in the N^+ case
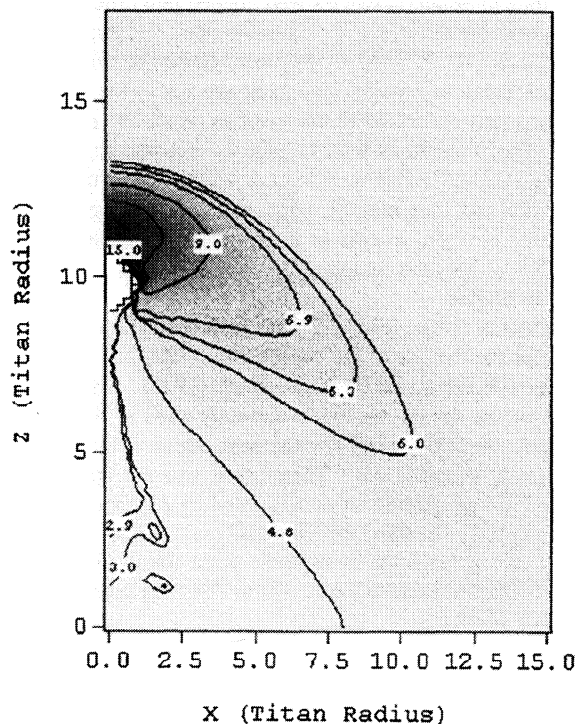

Figure 3. The magnitude of B for the $C_2H_5^+$ simulations show in the plane containing the flow and the magnetic field vector. Labels are in nanoteslas.
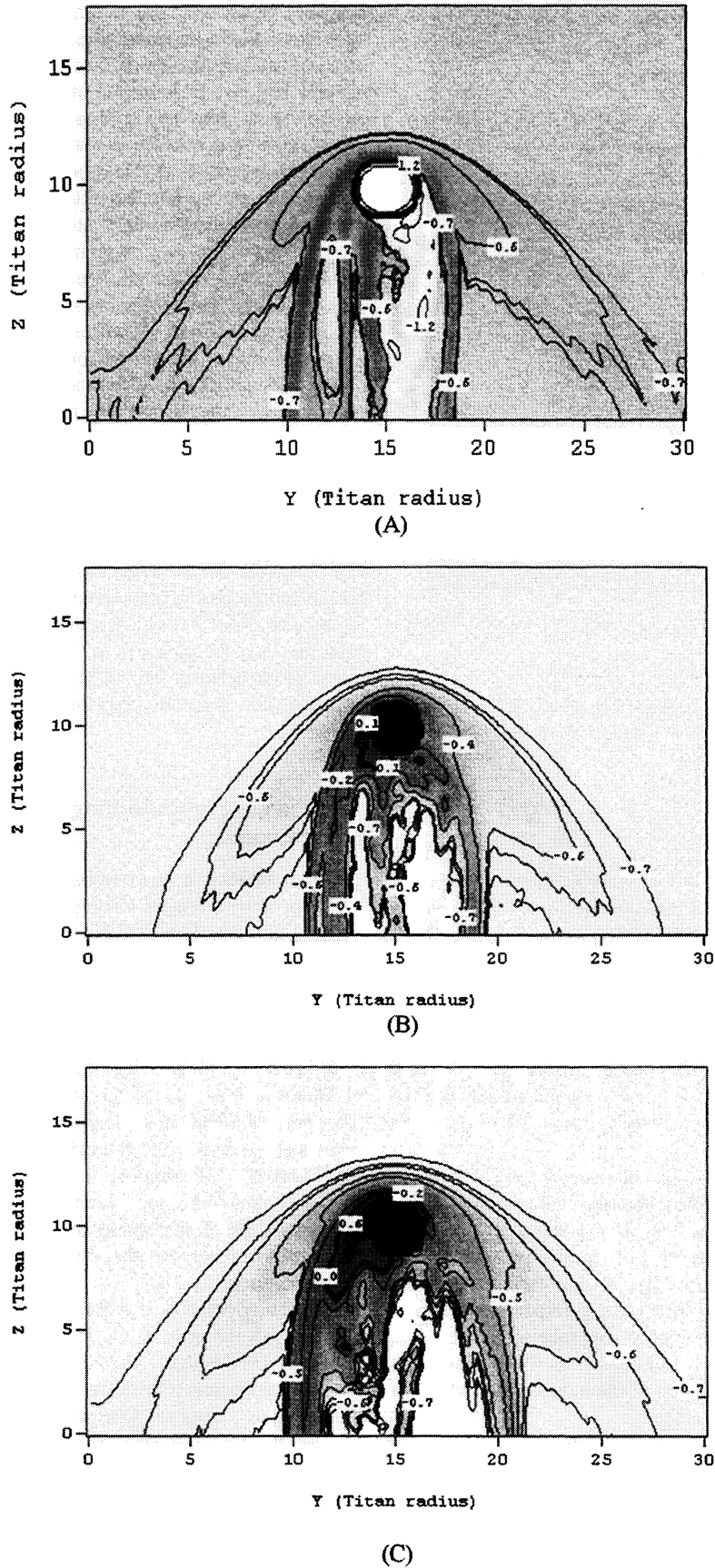
(A)

(B)

(C)

Figure 4. Contour plots of the ion density flow and convection electric field plane for the (a) H^+ load, (b) N^+ load, and (c) $C_2H_5^+$ load. Labels are log10 of density.
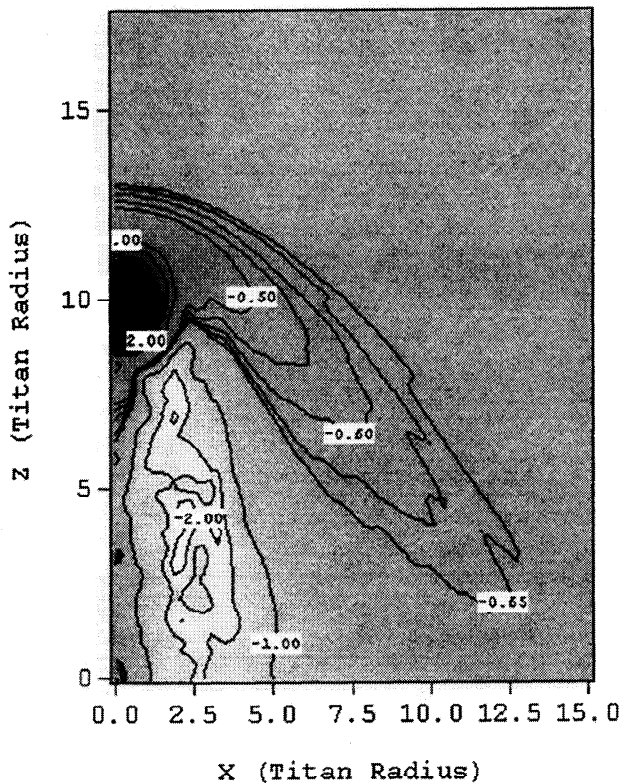
Figure 5. Contour plot of ion density for the $C_2H_5^+$ load in the plane containing the plasma flow (-z) and the magnetic field vector (+x). Labels are log10 of density.

the clean boundary on the $+E_{conv}$ side of Titan is more diffuse. Finally, in the $C_2H_5^+$ case shown in Figure 4c, one sees the same asymmetric pickup of the ions with a more diffuse boundary on the $+E_{conv}$ side of Titan. The entire tail region is wider than the other cases. These results suggest a strong ion gryoradius effect at work. The orthogonal plane of the $C_2H_5^+$ case is considered in Figure 5, where the magnetic field and flow vectors are in the plane of the plot. Because all three cases appear very much the same, we do not show the N^+ and H^+ load results. An interesting feature seen in the plot of this plane is a bite-out region of the ionosphere just below the terminator line. This suggests that tail-ray-type structures are a possibility.

The behavior of the tail or wake regions of Titan can be compared to the more heavily studied Venusian tail region. The ion wake of Venus as observed by the plasma instrument on PVO included several classes of wake ions. There is a low-energy "tail ray" component that seems to arise from pickup from the terminator upper ionosphere and shows little finite gyroradius effect [*Luhmann*, 1993] and a higher-energy exospheric pickup ion component [*Moore et al.*, 1990]. The manner in which these populations participate in the production of the induced magnetotail is not understood [e.g.,*Tanaka*, 1993].

A more illuminating way to examine the role of the pickup ions is to look at the position of the particles at a particular time in a scatterplot. In Figures 6a-6c the particle locations are plotted in the plane containing the flow vector and the convection electric field. The left-hand panels show the external flow ions, N^+, plotted every fifth particle. The right-hand panels show the mass-

loaded ionospheric pickup ions. In Figure 6a one sees a very sharp boundary between the tail regions and the flanks. The boundary might be called a magnetopause if this were a planet. One also sees strong interpenetration of the external flow and pickup ions in the bow regions. Examination of the electric and magnetic fields on the flanks show two pickup mechanisms at work. On the $+E_{conv}$ side the convection electric field pulls the pickup ions away from the moon. On the opposite side the $E \times B$ drifts appear to make the pickup ions move in a tailward fashion. However, there are some complex field patterns in the tail region. There is some mixing in the $-E_{conv}$ region but a region devoid of flow ions in the $+E_{conv}$ side of the tail. This region is populated with pickup ions. In the N^+ mass-loaded case, Figure 6b, there appears to be less interpenetration of plasma on the bow side but more symmetric positioning of the pickup ions in the tail. The pickup ions appear to dominate throughout the tail region. Figure 6c shows the mixing of the external flow ions and the $C_2H_5^+$ ions. Here the tail structure is wider as seen in the magnetic field and total density plots. In the bow and flank regions one sees exclusion of the flow ions on the $-E_{conv}$ side of Titan and interpenetration on the $+E_{conv}$ side of the bow region.

In all cases the tail structure is not symmetric. There is a definite preference for the system to put the flow ions on one side of the tail and the pickup ions on the other. The inner part of the nose region also shows a very asymmetric pileup of magnetic flux. The flow ions and the pickup ions do not interpenetrate as much as might be expected in the tail region. This is reminiscent of the Mars situation as reported by *Lundin et al.* [1990a] and *Dubinin et al.* [1991].

4. General Flow and Magnetic Fields: Asymmetric Mass Loading

In this subsection we examine the effect of moving the location of the peak of the mass loading away from the direction of the external flow ram face of Titan. Four additional simulations were performed, each with the same ionospheric profile but the hemisphere of maximum production moved toward the flanks. The method of referring to these simulations is as follows: 90° is the side of Titan where the $+E_{conv}$ is pointing away from the surface, 180° is on the midnight side of the planet, and 270° is on the side of Titan where the E_{conv} is pointing into the surface of the planet. The four additional simulations all used $C_2H_5^+$ as the ionospheric constituent and used the following angles for loading: 70°, 90°, 270°, and 290°. Depending on whether magnetospheric electron impact or photoionization is dominant, the 290° case is most representative of the Titan position at the time of the Voyager 1 closest approach. However, the other cases provide a more complete set of possible options for Titan.

The major result is that having the flow direction vector not aligned with the peak of the ionization profile produced significantly different results. Figure 7 shows the density contours for the 270° simulation. Comparing this figure with Figure 4c shows a considerable difference. The magnetic field in the bow and outer regions, on the other hand, do not seem to respond much to the change of the ionization peak position. The magnetic fields are similar. However, the particle plots illustrate the differences in a very dramatic way. Figure 8 shows the flow and pickup ions for the 270° case. The comparison with the cases described earlier shows a larger rotation of the tail structure due to the different
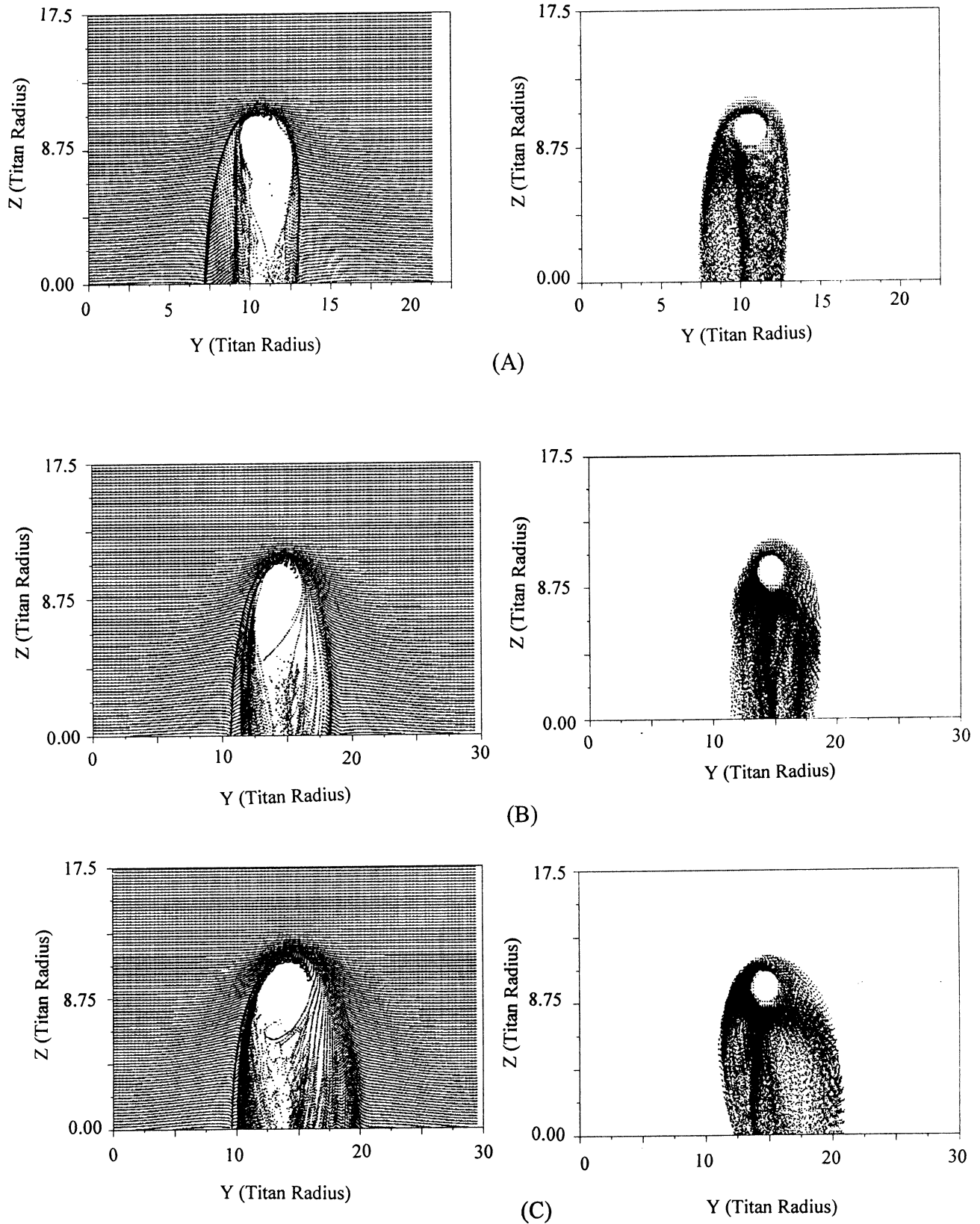
Figure 6. Particle position plots for the three load cases, showing (left) N^+ flow ions and (right) mass-loaded ions for (a) H^+, (b) N^+, and (c) $C_2H_5^+$ ions.
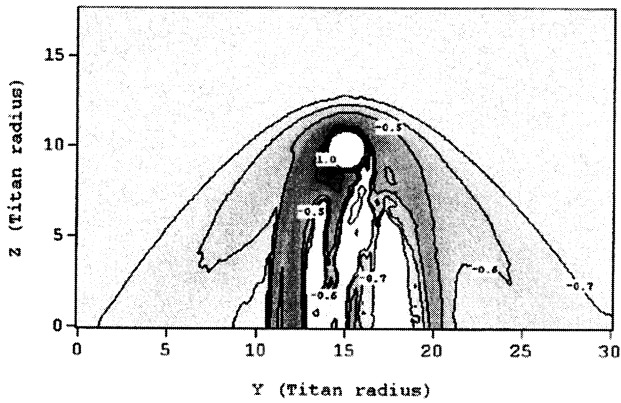
Figure 7. Total ion density contours shown in the plane containing the flow vector and the convection electric field. Labels are log10 of density.

mass loading pattern. The other simulations produce similar changes to the structure of the tail and the location of the pickup ions.

As will be discussed in subsequent paragraphs, the magnetic field profile measured by Voyager 1 had much sharper transitions than the simulations produced. There are several possible explanations for this difference, but two are the lack of sufficiently strong mass loading and high enough spatial numerical resolution. To examine this further, we picked up the N^+ simulation at step 7200 and restarted it with a mass loading rate stronger by a factor of 10. This brought the ionospheric densities to levels comparable to the peak densities calculated by *Keller et al.* [1992, 1994]. The results did not change appreciably, suggesting that better resolution of the ionosphere will be required for better comparisons with the data.

It will be seen that during the Voyager 1 flyby, the interaction between Titan and the flowing plasma appears to be controlled more by photoionization than by impact ionization produced by
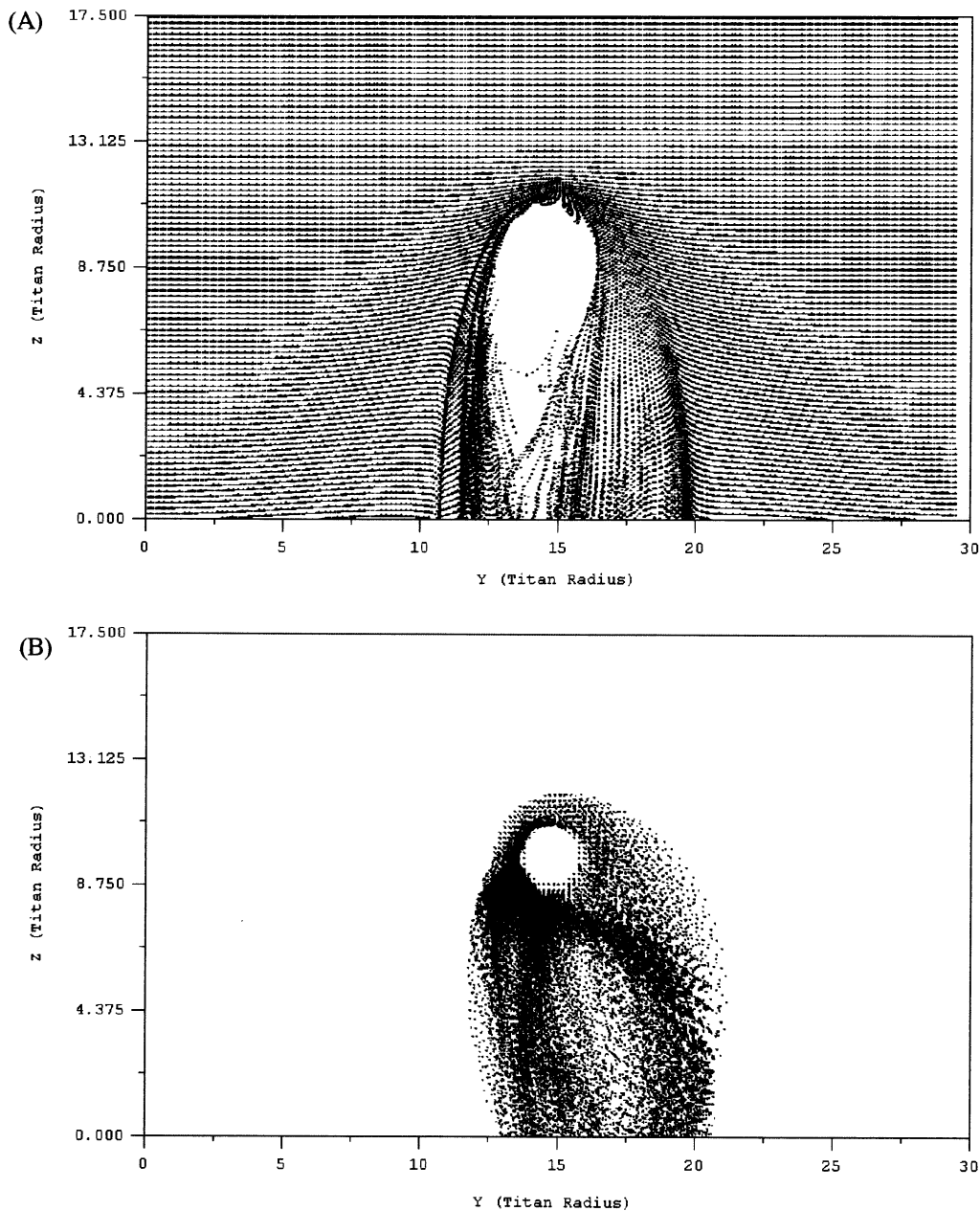

Figure 8. Particle positions for the 270° case in the plane containing the plasma flow vector and the convection electric field showing (a) N^+ plasma flow ions and (b) pickup ions, $C_2H_5^+$.
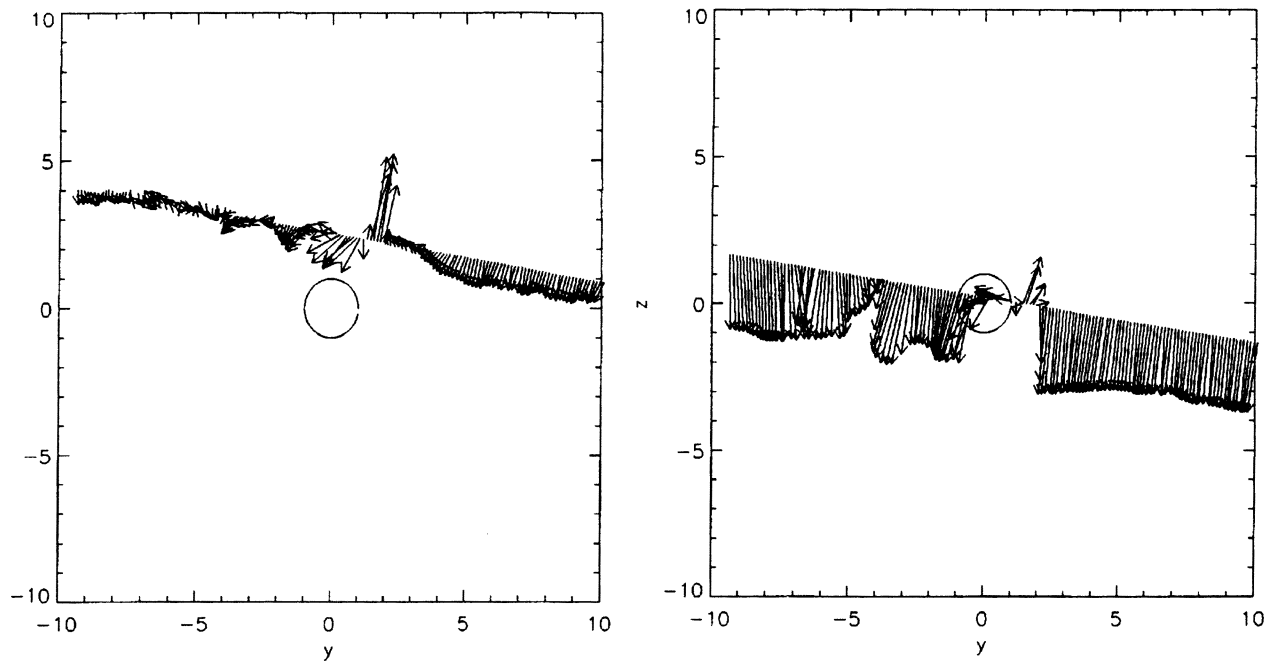
Figure 9. Magnetic vector plots from Voyager 1 flyby as reported by *Ness et al.* [1982].

the magnetospheric plasma. This conclusion is based on the comparison of the Voyager 1 flyby data with the simulations results.

5. Comparison to Data

The only data currently available on Titan's interaction with the Saturnian magnetosphere are those taken by Voyage 1 during a single flyby. Figures 9 and 10 show these data in the form of plots of the magnetic field [from *Ness et al.*, 1982] and electron density [from *Hartle et al.*, 1982], respectively, as the spacecraft passed across the tail region of Titan. The Voyager 1 trajectory was used to "fly" through the HALFSHEL simulations in order to make comparisons between the simulations and the data. Because it was found that the simulations using pickup $C_2H_5^+$ provided the best overall agreement, we show only that case here.

Figures 11 and 12 show the results of "flying" through the simulations where the peak ionization was collocated with the magnetospheric plasma ram face. The magnetic field vectors in Figure 11 generally agree with the data from Voyager 1. However, the sharp

transitions seen in the data are not found in the simulations. More interesting is the simulated density time series in Figure 12, where the peak density is found after closest approach (CA) rather than before as in the data. However, the features and magnitude of the density peak agree quite well.

In Figure 13 the results of flying through the simulations where the peak ionization is not collocated with the plasma ram face of Titan are seen. The magnetic field vectors did not change substantially from the previous cases and had the same general qualitative agreement with the data. However, the simulated density time series have now moved toward the CA and to the other side of the CA in better but not exact agreement with the Voyager 1 data.

Given the lack of resolution and approximate treatment of the ionosphere profiles, it is unlikely that very close agreement would be reached. However, these comparisons suggest that the tail region of Titan during the Voyager 1 flyby is controlled by photoionization rather than the electron impact ionization produced by the magnetospheric plasma. They also suggest that the tail region is very sensitive to the position of Titan in its orbit with respect to
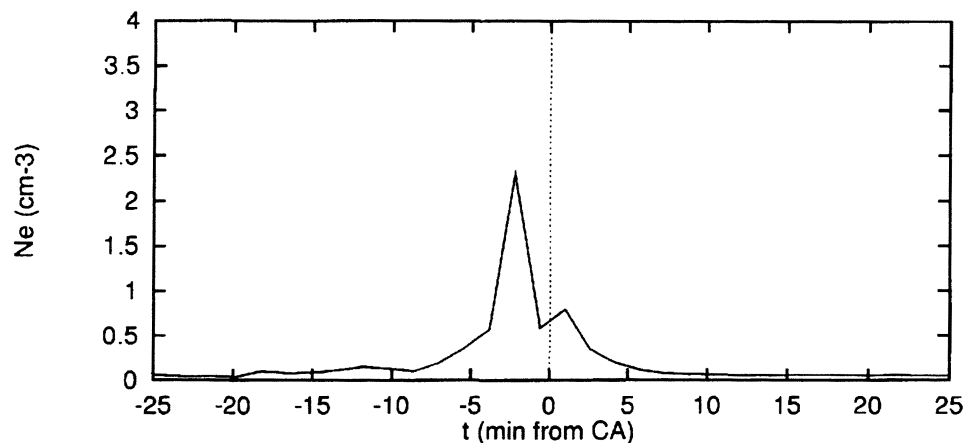

Figure 10. Plasma density time series from Voyager 1 flyby as reported by *Hartle et al.* [1982].
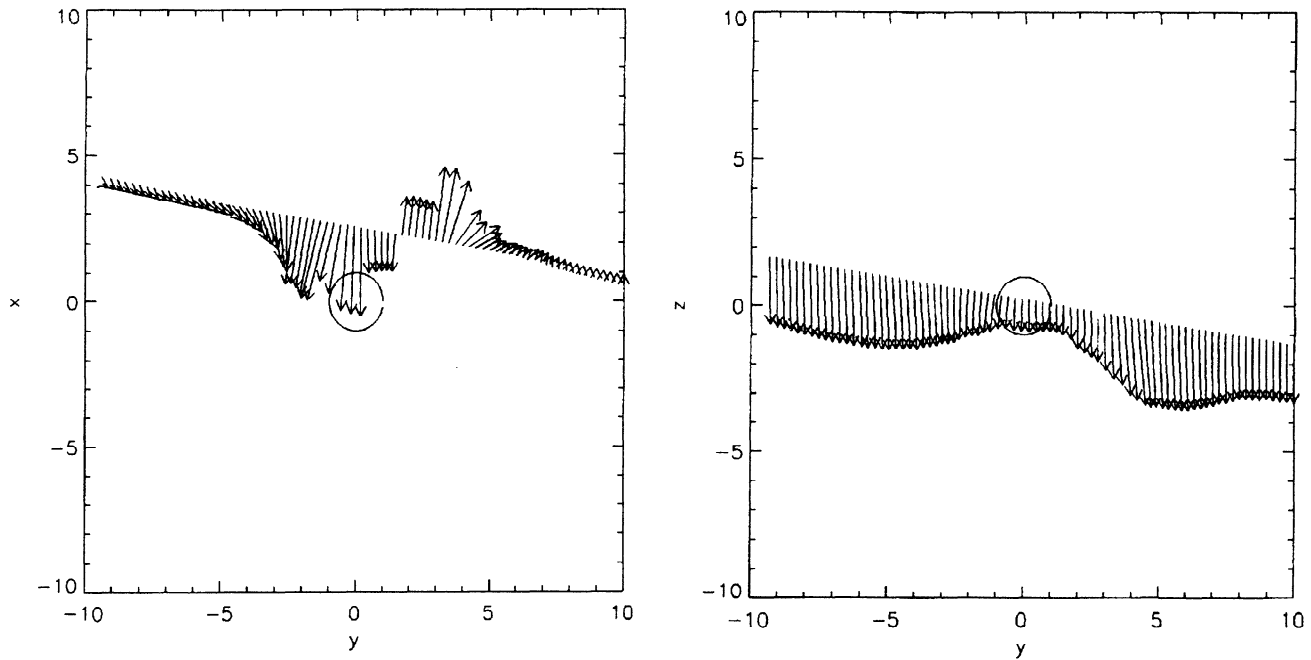
Figure 11. Simulated time series magnetic vector for centered mass loading of $C_2H_5^+$.

the Sun. It is notable that the shift of the Titan wake structure with respect to the corotation direction observed on Voyager 1 was attributed to a deflection of the oncoming plasma flow in earlier data analysis [e.g., *Kivelson and Russell*, 1983]. Here we obtain wake deflections of the right order simply by including the kinetic effects of the ions.

Several MHD models of the Titan interaction with Saturn's magnetosphere were also used to simulate the Voyager 1 flyby data [*Ledvina and Cravens*, 1998; *Kabin et al.*, 1999]. For the symmetric ionospheric mass loading cases shown in the literature, no wake deflection from the flow axis was obtained by the MHD simulations. While we cannot say how much wake deflection would be introduced by asymmetric ionosphere loading in the MHD models, we suspect that because the finite ion gyroradius and diamagnetic effects are absent, they will be weaker than those obtained with the HALFSHEL code which matches the Voyager 1 data reasonably well.

6. Conclusions

The simulations reported in this paper used the hybrid particle code approach to examine the effect of ion kinetics on the Titan interaction with Saturn. In these simulations the mass loading was accomplished using different Titan ion species. We investigated the effects of ionospheric/exospheric mass loading by different ion species and different source locations of the ionization (magnetospheric plasma impact versus solar EUV). It was found that the mass of the pickup ions made a notable difference in the features of the tail region of Titan. It was also concluded based on the enhanced mass-loaded N^+ simulation that the gyroradii of the ions in the pickup regions are very important to the structure of the Titan interaction with the magnetospheric flow. The major difference was in the width of the tail region. Further, the sharpness of various boundaries as seen to change with the different mass and ion gyroradii of the pickup ion species. In all cases the tail region
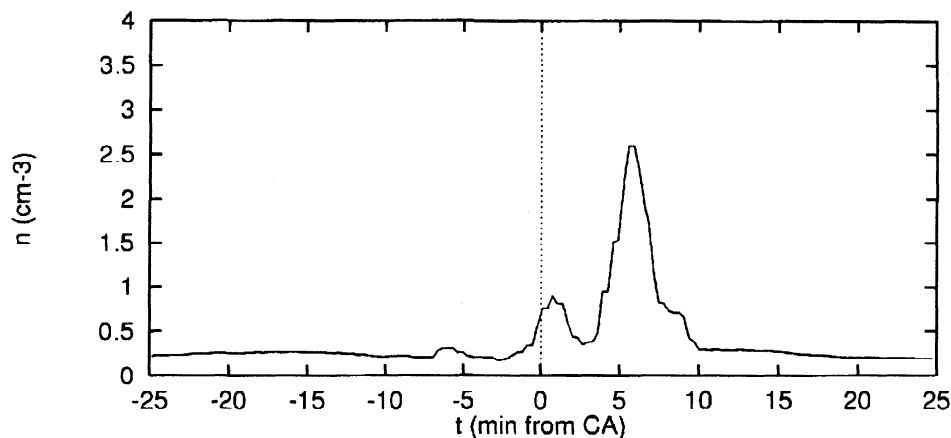

Figure 12. Simulated time series plasma density for centered mass loading of $C_2H_5^+$.
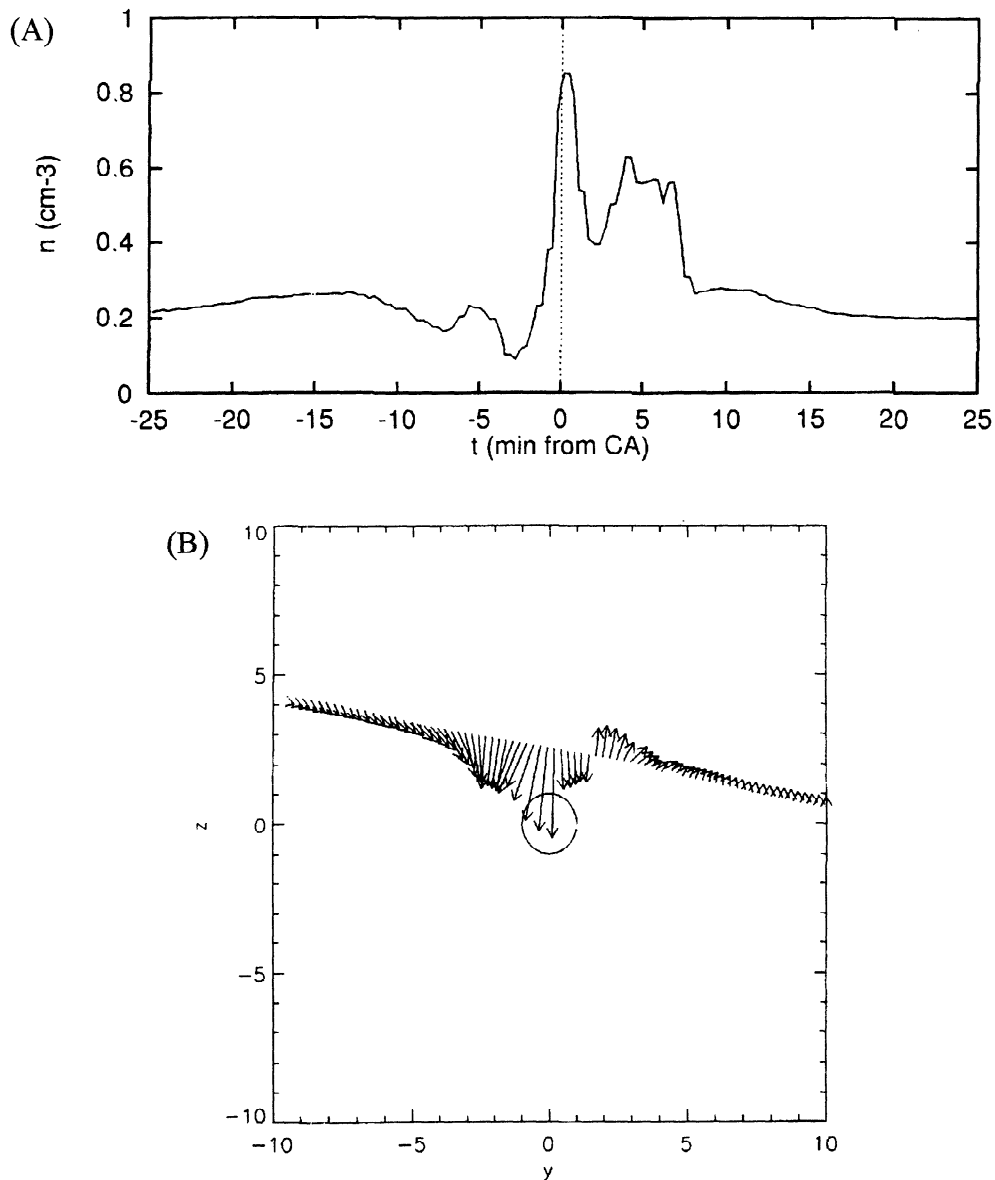
(A)

(B)

Figure 13. Simulated time series from 270° mass loading case of $C_2H_5^+$ (a) mass density and (b) time magnetic vector.

showed considerable density structure. Interestingly, the change in the total mass loading by virtue of holding the density profile constant for the different species made little difference to the overall magnetic structure surrounding Titan.

A particularly important result was obtained by moving the hemisphere of maximum ionization around Titan. It was found that the magnetic profiles did not change. However, the density profiles did change. This result reflects the effect of the large ion gyroradii of the mass-loaded hydrocarbon. The differences in the detailed trajectories of the pickup ions that cause these shifts will require more sophisticated analysis of the results than we are currently capable of performing.

The comparison of the results with the Voyager 1 data provided interesting insights into the actual interaction of Titan with Saturn's magnetosphere at that time. First, the simulation results compare favorably with the vector magnetic data from Voyager 1. This agreement occurs without regard to the choice of the pickup ion mass or ionization peak location. It should be mentioned that

the H^+ load case showed more wave action than the other cases. In some ways it seemed more reminiscent of the Voyager 1 data, but there are also waves in the magnetosphere of Saturn that could account for the variation seen in the data. The simulations never produced as sharp a rotation of the magnetic field as measured by the Voyager 1 spacecraft in the wake owing to the spatial resolution used in these initial simulations.

The comparisons with the density time series measured during the Voyager 1 flyby were surprising. Most of the simulation results have the peak density on the opposite side of closest approach from that in the Voyager 1 plasma data. However, the magnitudes and shapes of the density peaks agree quite well with those measured by Voyager 1. Changing the peak ionization location to the sunlit face of Titan during the Voyager 1 flyby moved the simulated density time series into better agreement with the observations. This suggests that the photoionization source is more important than the impact ionization source in determining the tail structure of Titan at the time of the Voyager 1 flyby. Given

the apparent sensitivity of the results to ionization source location, future simulations may require two ion production sites: one for photoionization and the other for the impact ionization.

These initial parameter studies of the Titan interaction with the Saturnian magnetosphere have illuminated a variety of areas where future simulations need to be improved. The asymmetric magnetic field pileup in the nose region and the shift of the tail structure away from the flow direction are indications of the diamagnetic interaction of Saturn's magnetospheric plasma with Titan. The type of ions being removed from the Titan ionosphere also makes a difference in the shape and size of the tail region of the Titan interaction, but the real situation is one of multiple pickup ion species and multiple ionization mechanisms. Agreement between the simulations and the data suggests that the heavy ion pickup is dominating the Titan system.

Finally, the extent to which the limited spatial resolution compromised the results cannot be completely appreciated. We plan in the near future to perform simulations with better resolution and more sophisticated ion production profiles. The analysis of these future simulations will include the display of detailed trajectories of the ions and their velocity and energy distribution functions as they may be observed on the Cassini mission orbiter.

References

Brecht, S.H., Magnetic asymmetry of unmagnetized planets, *Geophys. Res. Lett.*, *17*, 1243, 1990.

Brecht, S.H., Solar wind proton deposition into the Martian atmosphere, *J. Geophys. Res.*, *102*, 11,287, 1997a.

Brecht, S.H., Hybrid simulations of the magnetic topology of Mars, *J. Geophys. Res.*, *102*, 4743, 1997b.

Brecht, S.H., and J.R. Ferrante, Global hybrid simulation of unmagnetized planets: Comparison of Venus and Mars, *J. Geophys. Res.*, *96*, 11,209, 1991.

Brecht, S.H., and V.A. Thomas, Multidimensional simulations using hybrid particle codes, *Comput. Phys. Commun.*, *48*, 135, 1988.

Brecht, S.H., J.R. Ferrrante, and J.G. Luhmann, Three-dimensional simulations of the solar wind interaction with mars, *J. Geophys. Res.*, *98*, 1345, 1993.

Breus, T.K., et al., The solar wind interaction with Mars: Consideration of Phobos 2 mission observations of an ion composition on the dayside, *J. Geophys. Res.*, *96*, 11,165, 1991.

Dubinin, E., R. Lundin, W. Reidler, K. Schwingenschuh, J.G. Luhmann, C.T. Russell, and L.H. Brace, Comparison of observed plasma and magnetic field structures in the wakes of Mars and Venus, *J. Geophys. Res.*, *96*, 11,189, 1991.

Gurnett, D.A., F.L. Scarf, and W.S. Kurth, The structure of Titan's wake from plasma wave observations, *J. Geophys. Res.*, *87*, 1395, 1982.

Harned, D.S., Quasineutral hybrid simulation of macroscopic plasma phenomena, *J. Comput. Phys.*, *47*, 452, 1982.

Hartle, R.E., E.C. Sittler., K.W. Ogilvie, J.D. Scudder, A.J. Lazarus, and S.K. Atreya, Titan's ion exosphere observed from Voyager 1, *J. Geophys. Res.*, *87*, 1383, 1982.

Ip, W.-H., Titan's upper atmosphere, *Astrophys. J.*, *362*, 354, 1990a.

Ip, W.-H., The fast atomic oxygen corona extent of Mars, *Geophys. Res. Lett.*, *17*, 2289, 1990b.

Ip, W.-H., Plasma interaction of Titan with the Saturnian magnetosphere: A review of critical issues, in *Proceedings of Symposium on Titan, Eur. Space Agency Spec. Publ., ESA SP-388*, 1992.

Kabin, K., T.I. Gombosi, D.L. Zeeuw, K.G. Powell, and P.L. Israelevich, Interaction of the Saturnian magnetosphere with Titan: Results of a three-dimensional MHD simulation, *J. Geophys. Res.*, *104*, 2451, 1999.

Keller, C.N., T.E. Cravens, and L. Gan, A model of the ionosphere of Titan, *J. Geophys. Res.*, *97*, 12,117, 1992.

Keller, C.N., T.E. Cravens, and L. Gan, One-dimensional multispecies magnetohydrodynamic models of the ramside ionosphere of Titan, *J. Geophys. Res.*, *99*, 6511, 1994.

Kivelson, M.G., and C.T. Russell, The interaction of flowing plasmas with planetary ionospheres: Titan - Venus comparison, *J. Geophys. Res.*, *88*, 49, 1983.

Ledvina, S., and T.E. Cravens, A three-dimensional MHD model of plasma flow around Titan, *Planet. Space Sci.*, *46*, 1175, 1998.

Luhmann, J.G., A model of the ionospheric tail rays of Venus, *J. Geophys. Res.*, *98*, 17,615, 1993.

Luhmann, J.G., Titans's ion exosphere wake: A natural ion mass spectrometer?, *J. Geophys Res.*, *101*, 29, 387, 1996.

Luhmann, J.G., C.T. Russell, K. Schwingenschuh and Y. Yeroshenko, A comparison of induced magnetotails of planetary bodies: Venus, Mars, and Titan, *J. Geophys. Res.*, *96*, 11,199, 1991.

Luhmann J.G., S.H. Brecht, J.R. Sprieter, S.S. Stahara, R.S. Steinolfson, and A.F. Nagy, Global models of the solar wind interaction with Venus, in *Venus II*, edited by S. W. Bougher, D.M. Hunter, and R.J. Phillips, p. 33, Univ. of Ariz. Press, Tucson, 1997.

Lundin, R., et al., Plasma composition measurements of the Martian magnetosphere morphology, *Geophys. Res. Lett.*, *17*, 877, 1990a.

Lundin, R., et al., Aspera/Phobos measurements of the ion outflow from the Martian ionosphere, *Geophys. Res. Lett.*, *17*, 873, 1990b.

Moore, K.R., D.J. McComas, C.T. Russell and J.D. Mihalov, A statistical study of ions and magnetic fields in the Venus magnetotail, *J. Geophys. Res.*, *95*, 12,005, 1990.

Moore, K.R., D.J. McComas, C.T. Russell, S.S. Stahara and J.R. Spreiter, Gasdynamic model of the Venus magnetotail, *J. Geophys. Res.*, *96*, 5667, 1991a.

Moore, K.R., V.A. Thomas, and D.J. McComas, A global hybrid simulation of the solar wind interaction with the dayside of Venus, *J. Geophys. Res.*, *96*, 7779, 1991b.

Ness, N.F., M.H. Acuna, K.W. Behannon, and F.M. Neubauer, The induced magnetosphere of Titan, *J. Geophys. Res.*, *87*, 1369, 1982.

Neubauer, F.M., Titan's magnetospheric interaction, in *Proceedings of Symposium on Titan, Eur. Space Agency Spec. Publ., ESA SP-338*, 1992.

Tanaka, T., Configurations of the solar wind flow and magnetic field around planets with no magnetic field: Calculation by a new MHD simulation scheme, *J. Geophys. Res.*, *98*, 17,251, 1993.

Zhang, M.H.G., and J.G. Luhmann, Comparison of peak ionosphere pressures at Mars and Venus with incident solar wind dynamic pressure, *J. Geophys. Res.*, *97*, 1017, 1992.

_____

S. H. Brecht and D. J. Larson, Bay Area Research Corporation, P. O. Box 366, Orinda, CA 94563. (brecht@hooked.net)

J. G. Luhmann, Space Sciences Laboratory, University of California, Berkeley, CA 94720. (jgluhman@ssl.berkeley.edu)